Neurochemical Research (2019) 44:1090–1100
https://doi.org/10.1007/s11064-019-02740-5

ORIGINAL PAPER

Cytosolic HMGB1 Mediates Autophagy Activation in an Emulsified Isoflurane Anesthesia Cell Model

Rui-zhu Liu[1] · Tao Li[1] · Guo-qing Zhao[1]

Received: 5 September 2018 / Revised: 22 January 2019 / Accepted: 23 January 2019 / Published online: 2 February 2019
© Springer Science+Business Media, LLC, part of Springer Nature 2019

Abstract

Inhalation anesthetic isoflurane may cause an increased risk of cognitive impairment. Previous studies have indicated that this cognitive decline is associated with neuroinflammation mediated by high mobility group box 1 (HMGB1). HMGB1 is released from cells and acts as a damage-associated molecule in neurodegenerative diseases. However, the effect of intracellular HMGB1 during emulsified isoflurane (EI) exposure is poorly understood. The purpose of this study was to investigate the effect of autophagy on neuroprotection, evaluate variation of HMGB1, and determine its role in autophagic flux after EI exposure in vitro. We observed that EI decreased cell viability in a concentration-dependent manner, accompanied by an increase in autophagic flux. EI exposure also elevates the HMGB1 level in cytoplasm. Further, cytosolic HMGB1 was necessary for autophagy by perturbing the beclin1-Bcl-2 interaction. Most importantly, autophagy induction by rapamycin alleviated EI-provoked cell injury, and HMGB1 knockdown induced autophagy inhibition, which exacerbated cell damage. Based on these findings, we propose that autophagic flux is sustained and upregulated in response to EI exposure by increased cytosolic HMGB1, and that autophagy activation serves as a protective mechanism against EI-induced cytotoxicity. Thus, the complex roles of HMGB1 make it pivotal in reducing EI-induced neuronal damage.

Keywords Autophagy · Emulsified isoflurane · HMGB1 · Neuroprotection

Introduction

Halogenated inhalation anesthesia is a widely used anesthetic method in clinical practice. Emulsified isoflurane (EI), a novel type of anesthetic, provides rapid anesthesia that is less environmentally polluting and negates the specific equipment requirements of inhaled isoflurane. However, although a commonly used anesthetic, isoflurane has been reported to induce neurotoxicity associated with cognitive impairment [1, 2]. Findings from previous studies showed that post-anesthesia cognitive impairment is associated with neuroinflammation, neural apoptosis, and abnormal protein deposition in neurons [3–5], and is widely recognized. In the context of neurodegenerative diseases, it was determined that high mobility group box 1 (HMGB1) released from cells either after cell death or by active secretion [6], resulting in increased levels of extracellular HMGB1 in diseases, including cognitive and memory impairments [7–9].

Autophagy, which is an evolutionarily conservative self-digestion process that serves as a clearance pathway [10], plays a key role in the central nervous system because of the post-mitogenic nature of neurons, making it difficult for them to eliminate accumulated proteins and impaired organelles [11]. Previous studies have shown that downregulation of autophagy may be a cause of cognitive decline and neurodegeneration.

HMGB1 is a DNA binding protein in the nucleus [9]. During cellular stress, it is translocated to the cytoplasm and can be secreted from the cell [6]. Following secretion, HMGB1 acts as a damage-associated molecular pattern (DAMP) molecule to activate innate immune receptors and immune cells to mediate inflammatory responses [12, 13], which are associated with many neurological diseases. Studies have also demonstrated that systemic administration of anti-HMGB1 improves cognitive impairment after surgery in older rats [14]. However, these data reflect that the majority of research on HMGB1 has focused on its extracellular functions in neurodegenerative conditions, despite it

✉ Guo-qing Zhao
zhaogq65@126.com

[1] Department of Anesthesiology, China-Japan Union Hospital of Jilin University, No.126, Xiantai Rd, Changchun 130000, China

concurrently being found in the cytosol under these conditions. Very little is known about cytosolic HMGB1 after anesthetic exposure. The indications showed that protein level of HMGB1 was altered during post-anesthetic cognitive decline. Here, we investigated the toxic effects of EI on neuron-like cells in vitro and examined changes of intracellular HMGB1 under EI exposure, with the intended aim to understand its contributions to EI-induced neurotoxicity.

Materials and Methods

Cell Culture

Human neuroblastoma cell line (SH-SY5Y cells) and rat high-differentiated pheochromocytoma cell line (PC12 cells) induced by nerve growth factor (NGF) were purchased from the cell bank of the Chinese Academy of Sciences. Well-differentiated PC12 cells could preserve dopaminergic characteristics and neuronal properties, which have been broadly studied as a cellular model of neurological disease [15, 16]. The cells were cultured in Dulbecco's modified Eagle's medium (HyClone, USA) containing 10% v/v heat-inactivated fetal bovine serum and 100 U/mL penicillin (Gibco, USA). Cells were incubated at 37 °C with 5% v/v CO_2 in a humidified incubator.

Drug Administration

Intralipid® (30% w/v) was obtained from Sino-Swed Pharmaceutical Crop. Ltd. (Wuxi, China), and EI (8% v/v) was manufactured by West China Hospital of Sichuan University (Chengdu, China.). In the pilot experiment, SH-SY5Y cells and differentiated PC12 cells were incubated with EI final concentration of 0.28, 0.56, 0.84, and 1.12 mM and 1.58 μL/mL intralipid as a vehicle for 24 h. Based on the results, in the following experiments cells were exposed to 0.79 μL/mL intralipid and 0.56 mM EI.

Cell Viability Analysis

SH-SY5Y and PC12 cells were seeded in 96-well plates then treated with intralipid or EI for 24 h. The cell viability was measured using cell counting kit-8 (CCK-8) assay according to its manufacturer's instructions. After exposure to drugs, 10 μL CCK-8 (Beyotime Biotechnology, Wuhan, China) was subsequently added to the culture medium and then continue to incubate for 1 h at 37 °C. Absorbance was measured at 450 nm on an Epoch plate reader (Bio-TekInstrument Inc., USA). The relative cell viability and the half maximal inhibitory concentration (IC50) were determined.

Western Blot

Total cellular protein was extracted using RIPA lysis buffer (P0013C; Beyotime Biotechnology, Wuhan, China). Nuclear and cytosolic proteins were also separately extracted using the Nuclear and Cytoplasmic Protein Extraction Kit (Beyotime Biotechnology) according to the manufacturer's instructions. Protein concentrations of the different supernatants were measured by BCA Protein Assay Kit (Beyotime Biotechnology). Approximately 30 μg of protein was separated by electrophoresis using 12% sodium dodecyl sulfate–polyacrylamide gels, then transferred to a nitrocellulose filter membrane (Whatman, Dassel, Germany). After blocking with 5% w/v skim milk at room temperature for 1.5 h, the membrane was then incubated with the appropriate primary antibody: anti-HMGB1 antibody (6893S; Cell Signaling technology, USA; 1:1000 dilution); anti-Beclin1 antibody (3495S; Cell Signaling technology, USA; 1:1000 dilution) and anti-p62 antibody (8025S; Cell Signaling technology, USA; 1:1000 dilution); anti-LC3A/B antibody (12741S; Cell Signaling technology, USA; 1:1000 dilution); anti-Caspase 3 antibody (9662S; Cell Signaling technology, USA; 1:1000 dilution); anti-Bcl-2 antibody (2872S; Cell Signaling technology, USA; 1:1000 dilution); and anti-GAPDH antibody (5174S; Cell Signaling technology, USA; 1:3000 dilution) overnight at 4 °C. Membranes were washed five times for 3 min with Tris-buffered saline-Tween 20 and then incubated with the appropriate secondary antibody at room temperature for 1 h. Bands were visualized using enhanced chemiluminescence solution (Santa Cruz Biotechnology, Dallas, TX, USA). Relative band intensities were quantified by Image J.

Apoptotic Cell Analysis and Cell Morphology

Indicated cells were cultured in six-well plates, followed by drug exposure for 24 h. The rate of cell apoptosis was examined by flow cytometry analysis. Briefly, harvested cells were resuspended in 1 × Annexin V binding buffer for 5 min, following stained by propidium iodide for 10 min at room temperature. The apoptotic ratio was determined by a Novocyte Flow Cytometer System (ACEA Biosciences, Inc., China). Cell morphology was observed using an AE2000 optical microscope (Motic, China) and images were captured using TCapture (Tengrant, China).

Transfection and LC3 Punctuation Assay

Dual fluorescent mRFP-EGFP-LC3 plasmid was transfected into SH-SY5Y and PC12 cells by Lipofectamine 3000 (Invitrogen, Waltham, MA, USA). Next, 24–48 h post-transfection, cells were exposed to EI for 24 h.

Cells treated with 5 mmol/L of 3-methyladenine (class III PI3K inhibitor, Selleck, USA) for 24 h were served as autophagy-negative controls. Cells treated with serum starvation, which was induced by DMEM containing 0.1% v/v heat-inactivated fetal bovine serum for 24 h, served as autophagy-positive controls. The cells were washed with phosphate-buffered saline (PBS) and fixed with 4% w/v paraformaldehyde for 30 min at room temperature. Image was captured by Cytation three imaging reader (Bio-Tek Inc.) using a standard filter set. The autophagosomes (yellow dots) and autolysosomes (red dots) were scored in 30–40 cells per group. Negative control (nc)-siRNA or HMGB1-siRNA (RiboBio Co. Ltd, Guangzhou, China) were transfected into SH-SY5Y cells by Lipofectamine 3000 according to the manufacturer's instructions.

Immunofluorescence

Cells were cultured in 24-well cell plates. After fixing in 4% w/v paraformaldehyde for 30 min, cells were permeabilized with 0.1% v/v Triton X-100 at room temperature for 15 min. Cells were blocked with 2% BSA at room temperature for 30 min, and then incubated with an anti-HMGB1 or anti-microtubule-associated protein2 (MAP2) (8707S; Cell Signaling technology, USA) primary antibody, followed by incubation with a fluorescein isothiocyanate-conjugated anti-rabbit IgG secondary antibody. Nuclei were stained by 4′,6-diamidino-2-phenylindole (Solarbio, Beijing, China) for 5 min. Between each step, cells were washed with PBS three times. Images were captured under a fluorescence microscope (Leica Microsystem Inc, Germany.).

Co-immunoprecipitation Analysis

Co-immunoprecipitation (Co-IP) was performed as described previously (Marquez and Xu, 2012). SH-SY5Y cell lysate containing 120 μg total protein was directly assessed by western blot, while the remaining cell lysate was prepared for co-IP. The negative control group consisted of normal cell lysates incubated with IgG. Primary antibodies (1:100 dilution) were added to 200 μL of cell lysate, and incubated with rotation overnight at 4 °C to form immune-complexes. The antibody-antigen complex was precipitated using 30 μL cell lysis buffer balanced protein A/G agarose (Santa Cruz Biotechnology), and then incubated for 3–4 h at 4 °C with rotation. Agarose beads were washed three times with RIPA lysis buffer (Beyotime), followed by addition of 1 × SDS loading buffer to elute proteins by boiling before sodium dodecyl sulfate–polyacrylamide gel electrophoresis.

Statistical Analysis

Data are expressed as mean ± standard (SD). Comparisons among groups were analyzed using one-way analysis of variance (ANOVA) followed by Tukey post hoc test. A P-value < 0.05 was considered statistically significant. All data were obtained from 3 to 6 independent experiments.

Results

Neuronal Properties of SH-SY5Y Cells and PC12 Cells, and EI-Induced Decrease of Cell Viability in a Concentration-Dependent Manner

MAP2, the neuron-specific cytoskeletal protein, is a marker of neuronal phenotype. Positive staining of MAP2 in SH-SY5Y and high-differentiated PC12 cells was shown in Fig. 1a, to confirm the general neuronal properties of SH-SY5Y and PC12 cells. SH-SY5Y and PC12 cells were exposed to intralipid or different concentrations of EI for 24 h. The cell viability was evaluated by CCK-8 assay after 24 h EI treatment. As shown in Fig. 1b, EI at concentrations of 0.28, 0.56, 0.84, and 1.12 mM decreased viability of SH-SY5Y cells by 9.7, 11.8, 22.8, and 34.7%, respectively. Similarly, we found a significant concentration-dependent decrease in viability of PC12 cells compared to untreated controls. We determined that the IC50 of EI was 1.614 mM in SH-SY5Y cells and 1.711 mM in PC12 cells.

EI Induces Autophagy in SH-SY5Y and PC12 Cells

The autophagy markers proteins LC3 (also known as MAP1LC3) and p62 were examined by western blot. The LC3-I (soluble form) converts to LC3-II (autophagosome-associated form) during autophagosome formation [17], while p62 is degraded in the autophagosome-lysosome pathway [18]. Following analysis of western blot, EI (0.28, 0.56, or 1.12 mM) significantly increased the ratios of LC3II/I by 1.2, 1.5, and 1.9-folds in SH-SY5Y cells and 2, 2.8, 3-folds in PC12 cells. Simultaneously, p62 protein levels were down-regulated by 1.2, 1.3, and 1.7-folds in SH-SY5Y cells and 1.6, 2.1, and 7.4-folds in PC12 cells, respectively (Fig. 2a, b). Additionally, to further confirm EI-induced increased autophagic flux, the plasmid mRFP-EGFP-LC3 was transfected into SH-SY5Y and PC12 cells. mRFP-EGFP-LC3 contains a dual fluorescent protein, it emits red fluorescence as a result of GFP quenching in an acidic environment indicating fusion between autophagosomes and lysosomes [19, 20]. Our results showed that EI exposure resulted in a significantly increased number of fully formed

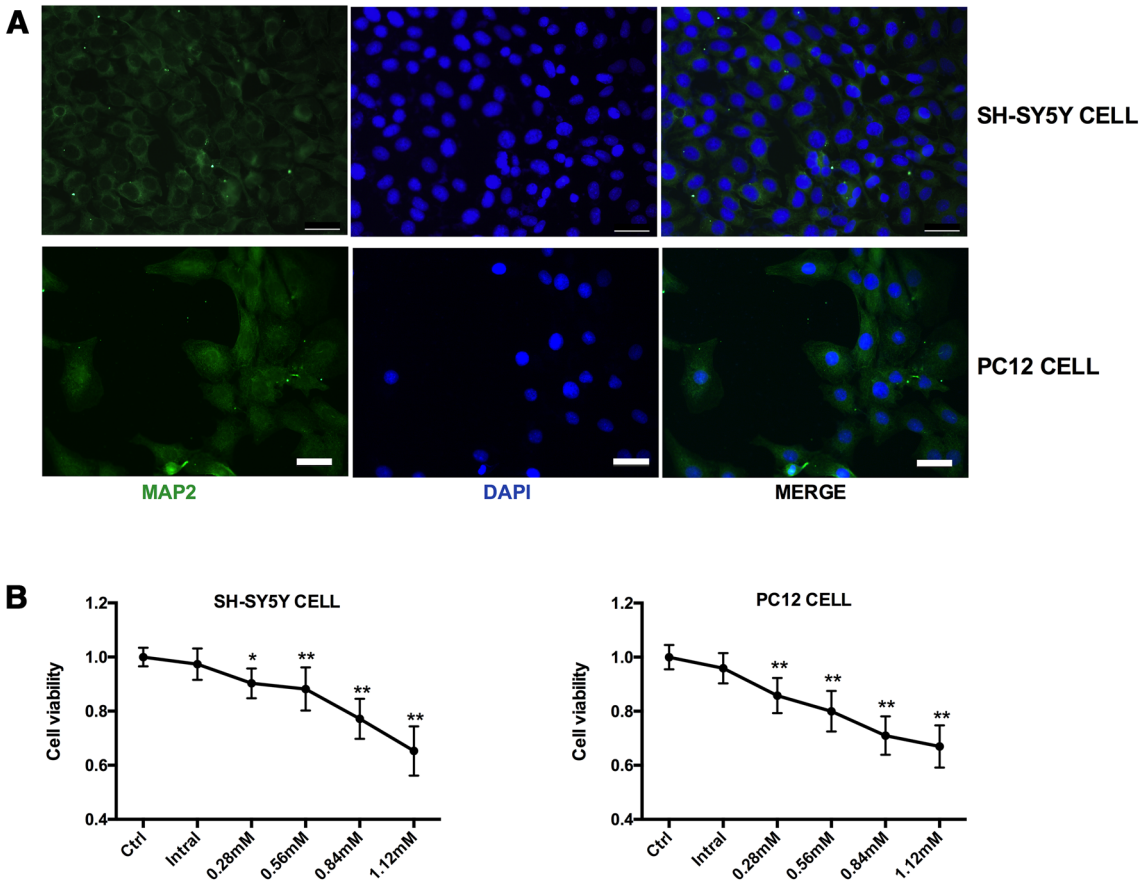

Fig. 1 Neurotoxicity of EI in SH-SY5Y and PC12 cells. **a** Fluorescence microscopic image of SH-SY5Y and differentiated PC12 cells stained by microtublule-associated protein 2 (MAP2). Scale bar = 100 μm **b** Concentration-effect relationship. SH-SY5Y and PC12 cells were challenged with 1.58 μl/ml intralipid or EI at the indicated concentrations for 24 h. Cell viability was evaluated by CCK-8 assay. *P < 0.05 and **P < 0.01 versus untreated controls; each experiment was performed 3–6 times. Ctrl: control; Intral: intralipid; EI: emulsified isoflurane

autophagosomes including both fused (red) and not fused (yellow) forms (Fig. 2c, d). These findings demonstrate that EI induced cell autophagy.

Autophagy Protects Against EI-Induced Apoptosis in SH-SY5Y and PC12 Cells

To determine the effect of autophagy in EI-induced apoptosis, SH-SY5Y and PC12 cells were co-treated with 1 μmol/L of rapamycin (mTOR inhibitor, Selleck, USA) [21] and 0. 56 mM EI for 24 h. As shown in Fig. 3a, b, after co-treatment with EI and rapamycin, the ratio of LC3II/I increased and p62 level decreased compared to that found with EI treatment alone, a finding which suggests autophagy in SH-SY5Y cells and PC12 cells was enhanced by rapamycin. In line with previous findings, our results also indicate that EI significantly increased the level of cleaved caspase 3 (Fig. 3c, d) as well as the apoptosis rate of SH-SY5Y cells and PC12 cells (Fig. 3e, g). However, administration of rapamycin down-regulated expression of cleaved caspase 3 protein (Fig. 3c, d), and attenuated the apoptosis (Fig. 3e, g). In addition, compared with EI exposure, co-treatment with rapamycin significantly increased cell viability in SH-SY5Y cells by 11%, and in PC12 cells by 10% (Fig. 3f, h).

Elevated Cytosolic HMGB1 by EI Exposure

HMGB1 protein levels in the cytoplasm and nucleus were investigated by fluorescence microscopy and then confirmed by western blot. Fluorescence imaging indicated that HMGB1 was mainly expressed in the nucleus and scarcely located in the cytoplasm. However, total HMGB1 expression levels were significantly elevated 24 h after EI exposure, with some shutting from the nucleus to the cytoplasm (Fig. 4a, b). Moreover, results of the western blot verified that HMGB1 was mainly localized in the nucleus in control (untreated) SH-SY5Y cells. Expression levels of HMGB1 significantly increased in both nucleus and

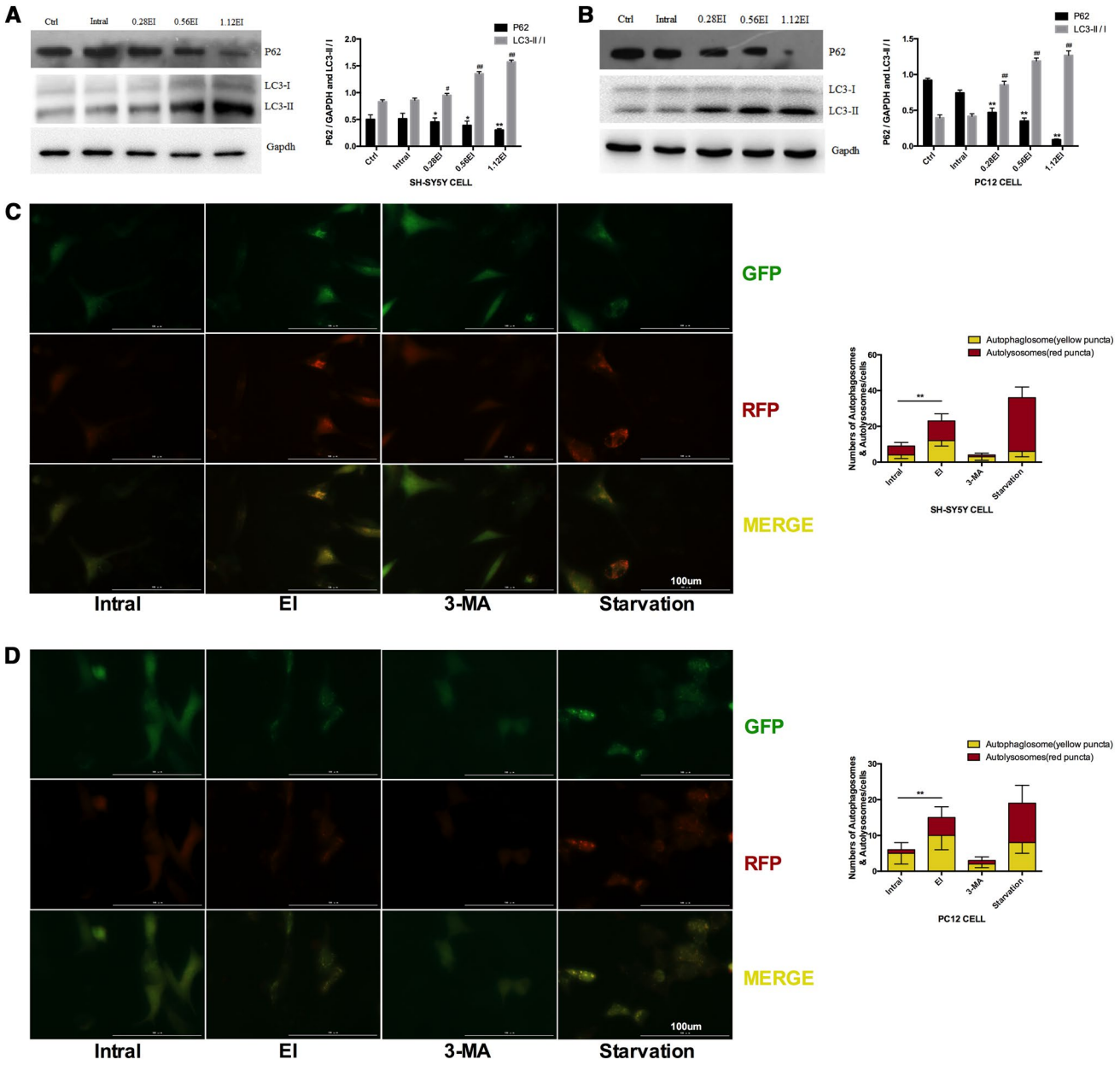

Fig. 2 EI increased autophagic flux in SH-SY5Y and PC12 cells. LC3-II/I and p62 levels in **a** SH-SY5Y cells and **b** PC12 cells. Cells were treated with EI for 24 h, untreated cells and intralipid-treated groups served as controls. Cellular extracts were prepared for western blot with antibodies against LC3 and p62. **c, d** Dual fluorescence LC3 assay. SH-SY5Y and PC12 cells were transiently transfected with a dual fluorescent (mRFP-EGFP) ptfLC3 plasmid. 24 h after transfection, cells were treated with EI for 24 h. Cells with serum starvation or with 3-methyladenine served as autophagy-positive and -negative controls, respectively. Scale bar = 100 μm. *#P < 0.05 and **##P < 0.01 versus controls; each experiment was performed 3–6 times. Ctrl: control; Intral: intralipid; EI: emulsified isoflurane; 3-MA: 3-methyladenine

cytoplasm after EI (0.28, 0.56 mM) exposure, the cytosolic HMGB1 levels were up-regulated by 28 and 55 folds in SH-SY5Y cells, by 8 and 20-folds in PC12 cells (Fig. 4c, d). Based on these findings, EI exposure results in over-expression of cytosolic HMGB1 in SH-SY5Y cells and PC12 cells.

HMGB1 Affects Cellular Morphology and Viability

To further investigate the effect of HMGB1 on EI-induced cell injury, HMGB1-siRNA and nc-siRNA were transiently transfected into SH-SY5Y cells with or without EI exposure. We found that HMGB1 protein was significantly elevated

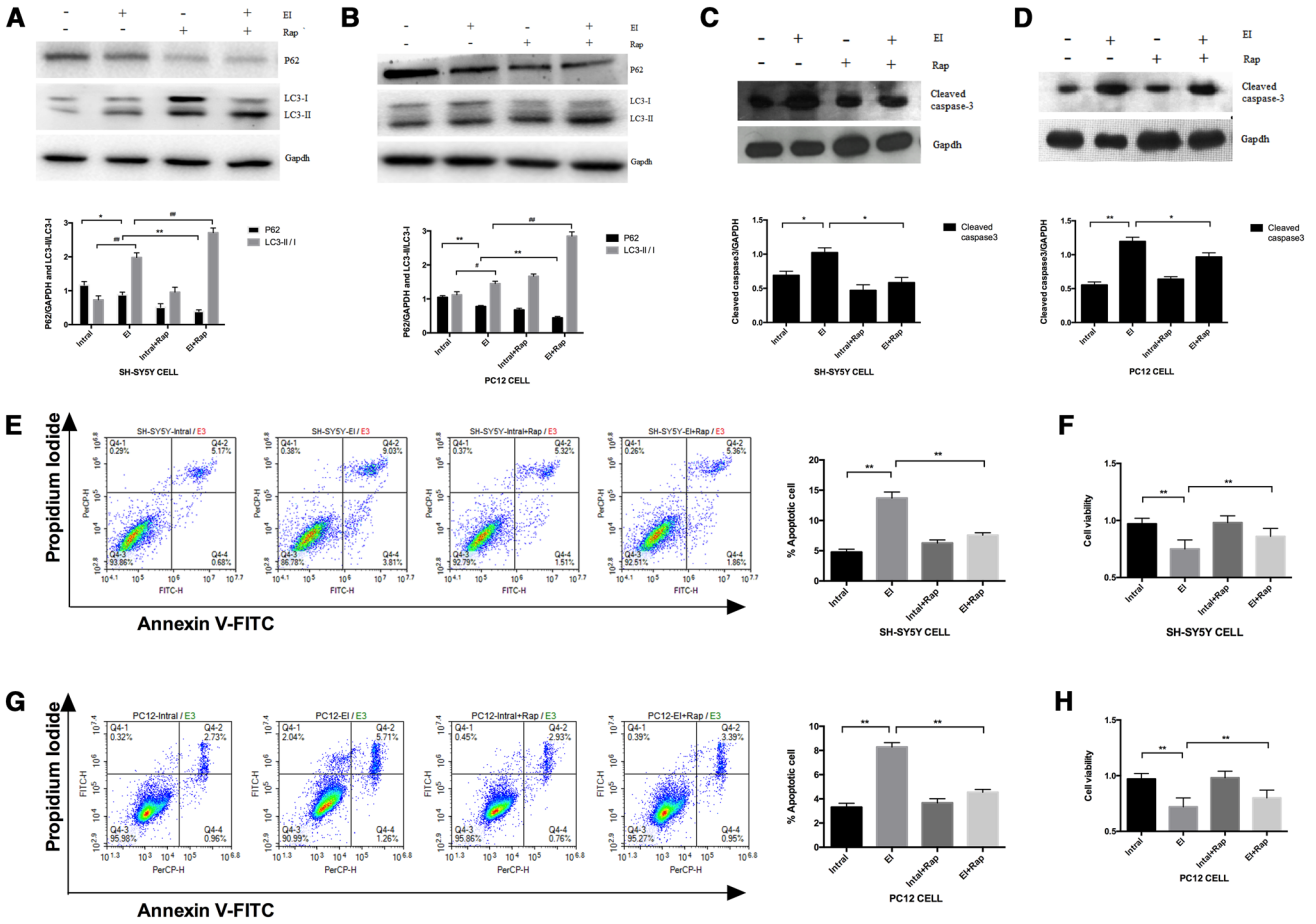

Fig. 3 Activation of autophagy prevents EI-induced apoptosis in SH-SY5Y and PC12 cells. LC3-II/I and p62 levels in **a** SH-SY5Y cells and **b** PC12 cells. Levels of cleaved caspase 3 in **c** SH-SY5Y cells and **d** PC12 cells. Cells from two cell lines were exposed to EI with/without 1 μmol/L rapamycin (Rap) for 24 h. Cells treated with intralipid served as controls. Apoptosis rate was assayed by flow cytometry using Annexin V-fluorescein isothiocyanate/propidium iodide staining in **e** SH-SY5Y cells and **g** PC12 cells. Effect of rapamycin on cell viability after EI treatment was determined by CCK-8 in **f** SH-SY5Y cells and **h** PC12 cells. Data are presented as the mean ± SD from 3 to 6 independent experiments. *#P < 0.05 and **##P < 0.01. Intral: intralipid; EI: emulsified isoflurane; Rap: rapamycin

after EI exposure, but that this EI-induced effect was lost with HMGB1 knockdown (Fig. 5a, b). However, distribution patterns of HMGB1 showed similar changes compared to earlier findings (Fig. 4a), regardless of HMGB1 knockdown (Fig. 5a). Morphological changes attributed to EI exposure namely cellular rounding, shrinkage, and contraction (Fig. 5c), were further exacerbated following HMGB1-siRNA transfection. The cleaved caspase 3 was further increased after EI exposure in HMGB1-silenced SH-SY5Y cells (Fig. 5b). In addition, knockdown of HMGB1 upregulatd EI-induced apoptosis rate (Fig. 5d), and exacerbated the decrease of cell viability (Fig. 5e).

HMGB1 Activated Cell Autophagy Via Perturbations in Beclin1-Bcl-2 Complex Formation

To elucidate the effect of HMGB1 on autophagy, we examined autophagic flux after HMGB1 knockdown. Compared to control, we found more red (fused) and yellow (not fused) fluorescence after a 24 h-incubation with EI in SH-SY5Y cells (Fig. 6a). However, this phenomenon was significantly suppressed by HMGB1 interference. To confirm the activation effect of HMGB1 on autophagy, we also examined protein levels of p62 and LC3II/I ratio. We found that knockdown of HMGB1

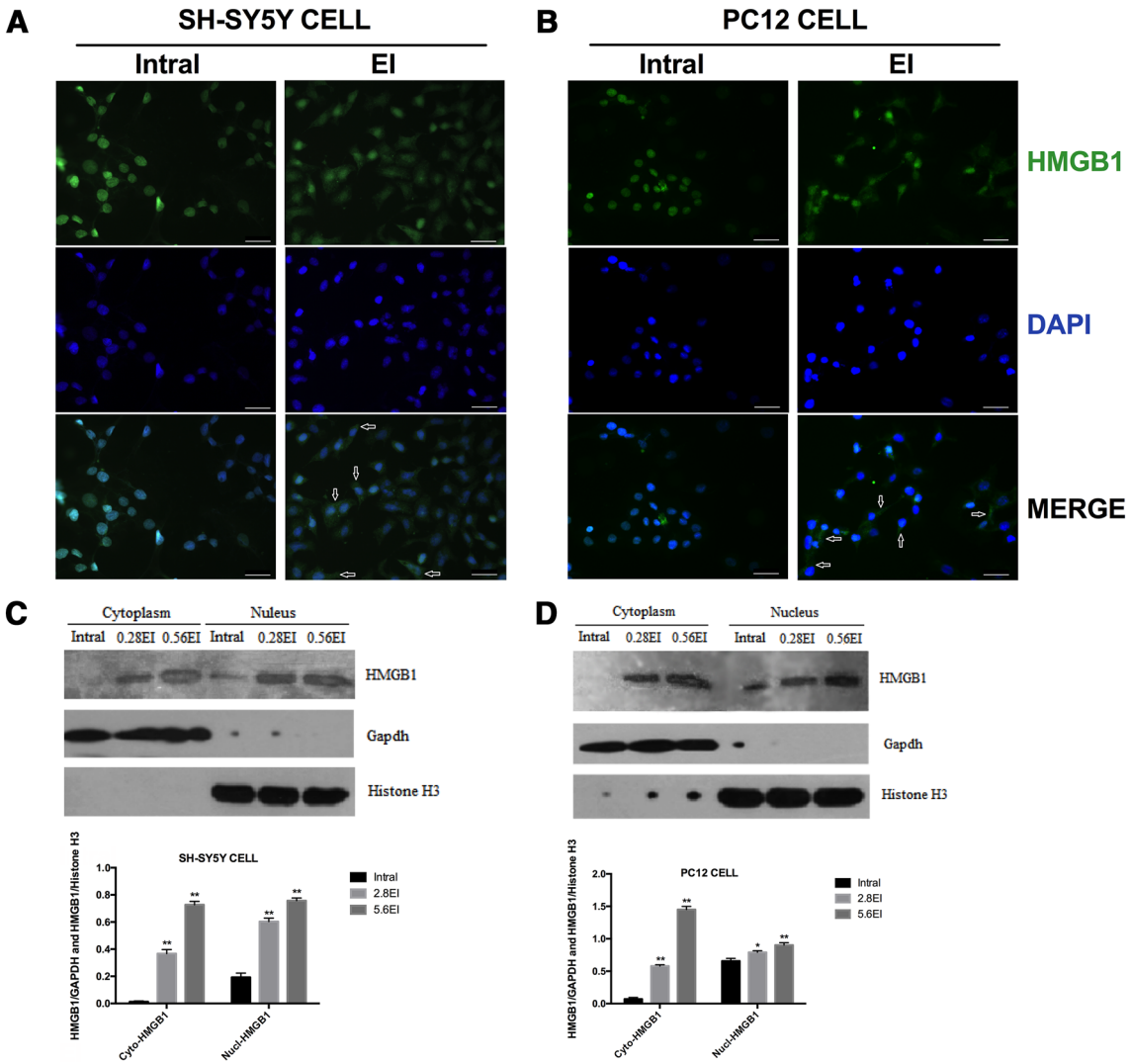

Fig. 4 Overexpression of HMGB1 upon EI exposure and translocation to cytoplasm in SH-SY5Y and PC12 cells. Overall HMGB1 expression increased with 0.56 mM EI treatment for 24 h, followed by cytoplasmic translocation (marked by arrows) as proven in fluorescence microscope (**a, b**). Scale bar = 100 μm. Cytoplasmic and nuclear HMGB1 protein levels were detected in SH-SY5Y cells (**c**) and PC12 cells (**d**). Data are presented as the mean ± SD from 3 to 6 independent experiments. *P < 0.05 and **P < 0.01. Intral: intralipid; EI: emulsified isoflurane

significantly reduced the EI-induced increased ratio of LC3II/I and degeneration of p62 (Fig. 6b). Analysis of co-IP showed that under normal conditions, endogenous beclin1 bound to Bcl-2 (Fig. 6c, d). However, EI exposure caused complex formation between beclin1 and HMGB1, resulting in dissociation of beclin1 from Bcl-2. Further, HMGB1 knockdown restored the complex formation between Bcl-2 and beclin1 in the cytoplasm (Fig. 6c, d). These findings indicate that HMGB1 has a high affinity for beclin1, which may activate and sustain the autophagy process through disassociation of the beclin1-Bcl-2 complex.

Discussion

The commonly used inhalation anesthesia, isoflurane, can induce neuronal loss and activation of neuroinflammatory signaling pathways, contributing to the anesthesia-associated inherent neurotoxicity [5, 22, 23]. In the present study, we investigated the endogenous self-defense mechanism in vitro, using SH-SY5Y cells and highly differentiated PC12 cells exposed to EI. We observed that EI induces an increase in the autophagic flux in SH-SY5Y and PC12 cells. The cytosolic HMGB1 is essential for

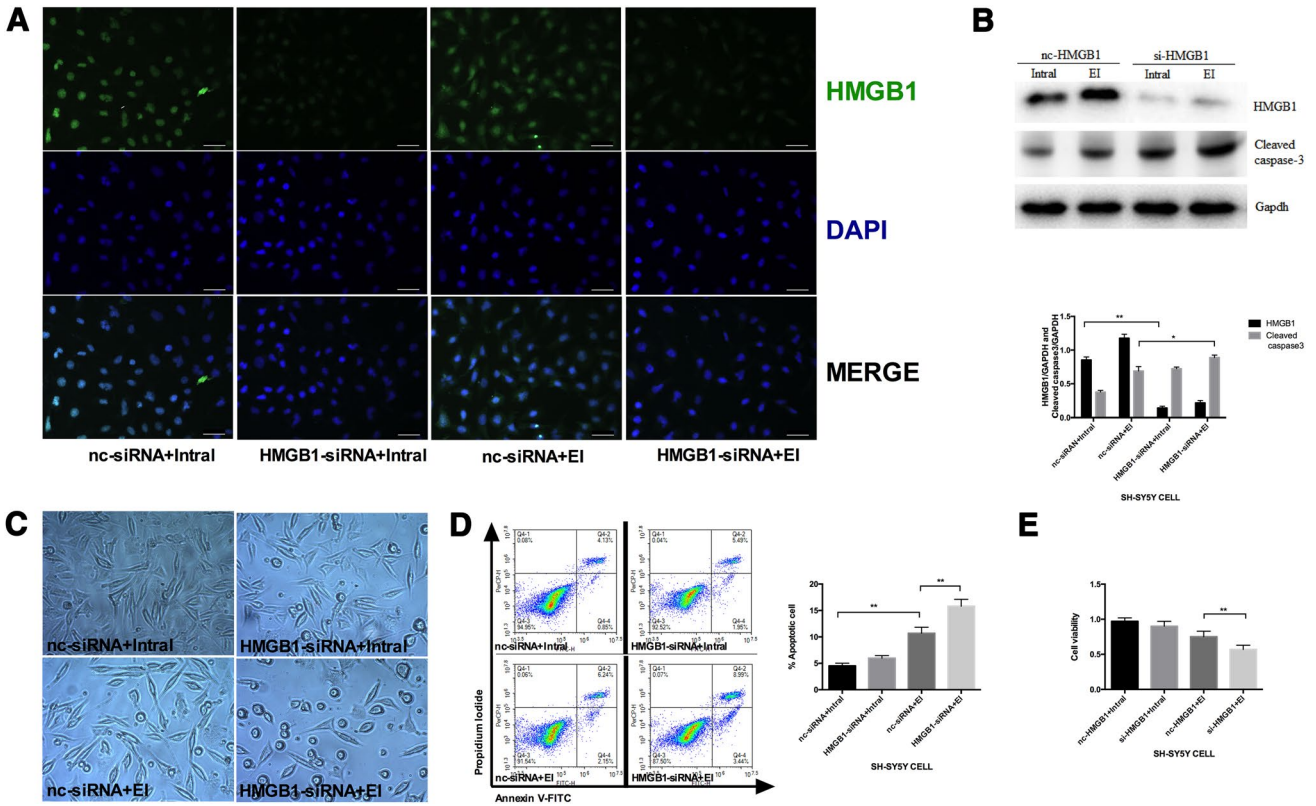

Fig. 5 Effects of HMGB1 on cellular morphology and viability. SHSY-5Y cells were transiently transfected with nc-siRNA or HMGB1-siRNA. **a** Fluorescence microscopy was used to detect HMGB1 expression and subcellular location after 24 h EI treatment (0.56 mM). Scale bar = 100 μm. **b** Expression levels of HMGB1 and cleaved caspase 3 were determined by western blot after siRNA transfection. Relative intensity was normalized to GAPDH. **c** Cellular morphology was observed following treatment with 0.56 mM EI after siRNA transfection under a phase-contrast microscope (×200 magnification). **d** Flow cytometry analysis of apoptosis rate in HMGB1-silencing SH-SY5Y cells. **e** CCK-8 analysis of cell viability in HMGB1-silencing SH-SY5Y cells. Data are presented as the mean ± SD from 3 to 6 independent experiments. *P < 0.05 and **P < 0.01. Intral: intralipid; EI: emulsified isoflurane

maintaining cellular autophagy, a process plays a protective role in EI-induced cell injury.

As determined in previous studies, autophagy has a dual pro-survival and pro-death role in cells. On the one hand, autophagy can take an alternative pathway interacting with apoptosis or necrosis as a combined mechanism for cell death [24]. On the other hand, many studies have demonstrated that autophagy plays a protective role in cells. In particular, in most acute and chronic neurodegenerative diseases, the process of autophagy is significant because of its role in diluting 'toxic assets' [25, 26]. Evidence has shown that an increase in autophagic flux was observed in ethanol and local anesthetic-induced neurotoxicity, whereas inhibition of autophagy potentiated oxidative stress and exacerbated cell injury [27, 28]. Recent investigations have also proposed that autophagy may be a potential way to alleviate post-anesthesia neurotoxicity [29, 30]. Consistent with previous studies, our results showed that autophagy could be triggered in an EI concentration-dependent manner, and the up-regulation of autophagic flux could effectively ameliorate the EI-induced cell injury (Fig. 3), which indicates a cellular self-defense response activated under EI exposure.

In response to stress, HMGB1 is released extracellularly and acts as a DAMP or "danger" signal, participating in many inflammatory processes, including general anesthetic-induced cognitive decline. Evidence has shown that activation of the HMGB1/NF-κB pathway under isoflurane exposure in vitro contributes to an increase in the pro-inflammatory cytokines [23]. Inhibition of HMGB1 could have a protective effect in isoflurane-induced neurotoxicity in vivo via attenuation of inflammation [31, 32]. However, knockdown of HMGB1 in the intestinal epithelial cells unexpectedly exacerbates acute and chronic colitis in mice [33]. In the context of inflammatory diseases, the data suggest that a lower HMGB1 level is closely associated with increased mortality in sepsis patients [34]. In the present study, the cytosolic HMGB1 level was upregulated in EI concentration-dependent manner. Loss of HMGB1 further increased the EI-induced activated caspase 3 level and the apoptotic rate in SH-SY5Y and PC12 cells.

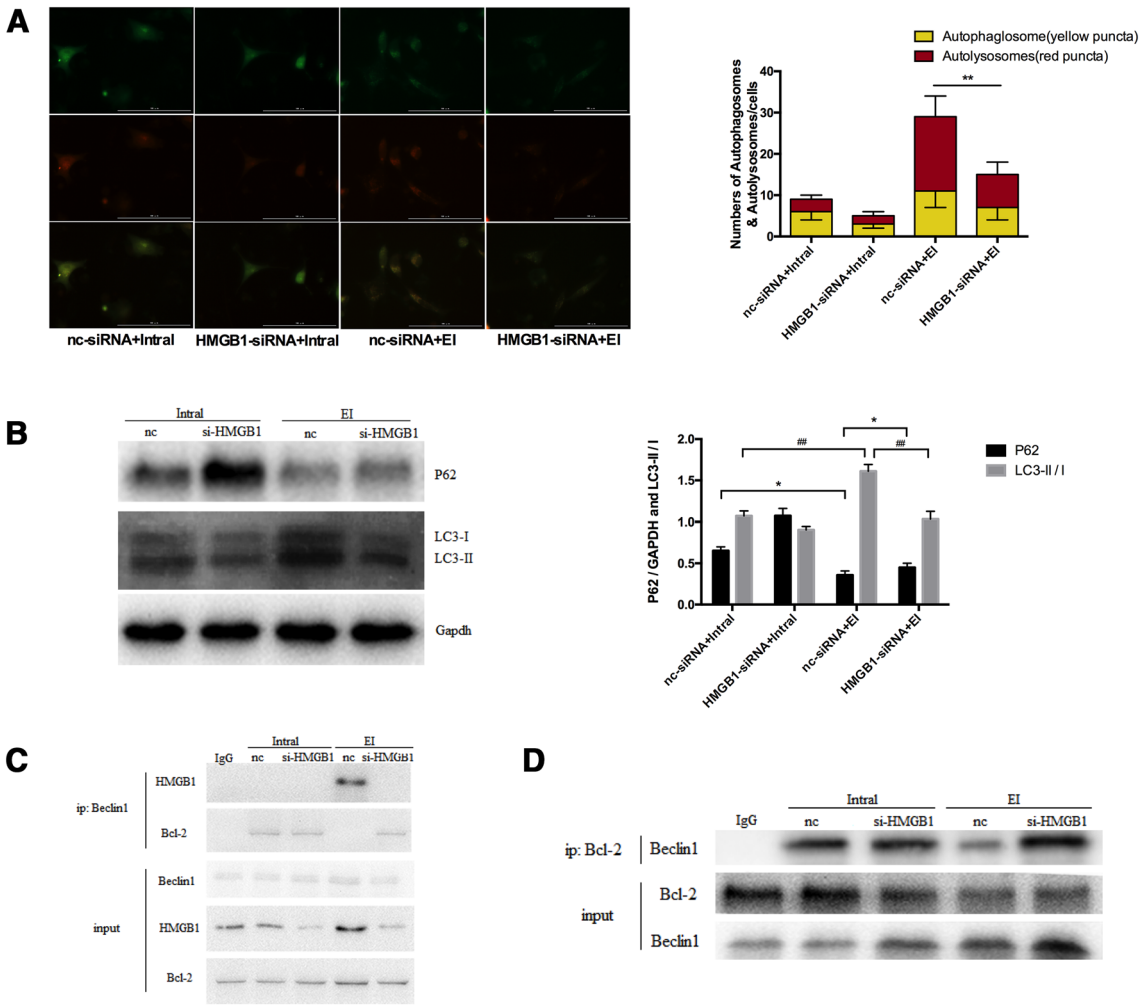

Fig. 6 HMGB1 mediated cellular autophagy via beclin1-Bcl-2 complex perturbation. SH-SY5Y cells were incubated with 0.56 mM EI for 24 h after ptf-LC3 plasmid and siRNA transfection. **a** GFP-LC3 puncta, RFP-LC3 puncta, and merged puncta were observed by fluorescence microscopy. Scale bar = 100 μm. **b** Western blot analysis of LC3II/I and p62 in HMGB1-silencing SH-SY5Y cells. **c** IP analysis of HMGB1-Beclin1 formation in HMGB1-silencing SH-SY5Y cells following EI exposure for 24 h. **d** IP analysis of Bcl2-Beclin1 formation in HMGB1-silencing SH-SY5Y cells following EI exposure for 24 h. Data are presented as the mean ± SD from 3 to 6 independent experiments. *#P < 0.05 and **##P < 0.01. Intral: intralipid; EI: emulsified isoflurane

Previous evidence and our results indicate that HMGB1 may play completely different roles depending on whether it is localized inside or outside the cell. Tang et al. [35] proposed that cytosolic HMGB1 serves as a pro-autophagic protein, which reveals a new role for HMGB1. A study has shown that HMGB1 is crucial for sustaining autophagy and for the degradation of α-synuclein in a Parkinson's disease PC12 cell model [36]. Additionally, endogenous HMGB1 could promote autophagic degradation via an ATG5-[37] and Beclin1-dependent autophagy pathway [33]. Consistent with previous studies, cytoplasmic HMGB1 could sustain autophagy via increased LC3II/I expression and p62 degradation, but the autophagic flux was significantly impaired in HMGB1-silenced SH-SY5Y cells under EI exposure. Upon EI exposure, cytosolic HMGB1 showed a higher affinity for Beclin1, which disrupted the Beclin1-Bcl-2 protein complex. Beclin1, as a protein interaction platform, is the pivotal component that balances autophagy-induced cytoprotective and cytotoxic effects [38]. The anti-apoptotic molecule Bcl-2, one of the Beclin1 binding proteins, is closely linked to the apoptotic and autophagic pathways that regulate cell survival and cell death. The dissociation of Beclin1 from Bcl-2 is a prerequisite for the activation of autophagy, and limits apoptosis in response to cellular stress [35, 39]. In fact, cellular autophagy is not affected in HMGB1-silenced hepatocytes under basal conditions [40]. However, under consistent cellular stress, such as that caused by EI exposure, the Beclin1-Bcl-2 protein complex not only inhibits autophagy initiation, but also causes an increase in apoptotic protein levels, and activates caspase 3 in HMGB1-silenced

SH-SY5Y cells. These finding indicate that HMGB1 is required for maintaining EI-induced autophagy, although the exact mechanism is not clear. When and how of the interaction between HMGB1 and Beclin1 in cytoplasm under anesthesia exposure require further investigation.

In summary, our findings demonstrate that EI-induced autophagy is a self-defense response. Elevation of cytosolic HMGB1 levels by EI exposure disrupts Beclin1-Bcl-2 complex formation and inducing autophagy. Thus, extracellular HMGB1 may act as a danger signal, while intracellular HMGB1 is required for the initiation of autophagy for cell survival. Our findings provide new insights into the potential cellular self-defense mechanisms in anesthesia-induced neurotoxicity.

Acknowledgements We would like to thank Dr. Shumei Ma at Jilin University for helping with experimental platform. We would like to thank Editage (http://www.editage.com) for English language editing.

Funding This work was supported by Natural Science Foundation of Jilin Province (Grant No. 3T1158303430). The funders had no role in study design, data collection and analysis, decision to publish or preparation of the manuscript.

Compliance with Ethical Standards

Conflict of interest All authors declare that they have no conflict of interest.

References

1. Bianchi SL, Tran T, Liu C, Lin S, Li Y, Keller JM, Eckenhoff RG, Eckenhoff MF (2008) Brain and behavior changes in 12-month-old Tg2576 and nontransgenic mice exposed to anesthetics. Neurobiol Aging 29(7):1002–1010. https://doi.org/10.1016/j.neurobiolaging.2007.02.009
2. Zhang Y, Xu Z, Wang H, Dong Y, Shi HN, Culley DJ, Crosby G, Marcantonio ER, Tanzi RE, Xie Z (2012) Anesthetics isoflurane and desflurane differently affect mitochondrial function, learning, and memory. Ann Neurol 71(5):687–698. https://doi.org/10.1002/ana.23536
3. Ge HW, Hu WW, Ma LL, Kong FJ (2015) Endoplasmic reticulum stress pathway mediates isoflurane-induced neuroapoptosis and cognitive impairments in aged rats. Physiol Behav 151:16–23. https://doi.org/10.1016/j.physbeh.2015.07.008
4. Lin D, Zuo Z (2011) Isoflurane induces hippocampal cell injury and cognitive impairments in adult rats. Neuropharmacology 61(8):1354–1359. https://doi.org/10.1016/j.neuropharm.2011.08.011
5. Shen X, Dong Y, Xu Z, Wang H, Miao C, Soriano SG, Sun D, Baxter MG, Zhang Y, Xie Z (2013) Selective anesthesia-induced neuroinflammation in developing mouse brain and cognitive impairment. Anesthesiology 118(3):502–515. https://doi.org/10.1097/ALN.0b013e3182834d77
6. Andersson U, Tracey KJ (2011) HMGB1 is a therapeutic target for sterile inflammation and infection. Annu Rev Immunol 29:139–162. https://doi.org/10.1146/annurev-immunol-030409-101323
7. Fang P, Schachner M, Shen YQ (2012) HMGB1 in development and diseases of the central nervous system. Mol Neurobiol 45(3):499–506. https://doi.org/10.1007/s12035-012-8264-y
8. Kang R, Chen R, Zhang Q, Hou W, Wu S, Cao L, Huang J, Yu Y, Fan XG, Yan Z, Sun X, Wang H, Wang Q, Tsung A, Billiar TR, Zeh HJ 3rd, Lotze MT, Tang D (2014) HMGB1 in health and disease. Mol Asp Med 40:1–116. https://doi.org/10.1016/j.mam.2014.05.001
9. Klune JR, Dhupar R, Cardinal J, Billiar TR, Tsung A (2008) HMGB1: endogenous danger signaling. Mol Med 14(7–8):476–484. https://doi.org/10.2119/2008-00034.Klune
10. Parzych KR, Klionsky DJ (2014) An overview of autophagy: morphology, mechanism, and regulation. Antioxid Redox Signal 20(3):460–473. https://doi.org/10.1089/ars.2013.5371
11. Tooze SA, Schiavo G (2008) Liaisons dangereuses: autophagy, neuronal survival and neurodegeneration. Curr Opin Neurobiol 18(5):504–515. https://doi.org/10.1016/j.conb.2008.09.015
12. Harris HE, Andersson U, Pisetsky DS (2012) HMGB1: a multifunctional alarmin driving autoimmune and inflammatory disease. Nat Rev Rheumatol 8(4):195–202. https://doi.org/10.1038/nrrheum.2011.222
13. Lotze MT, Tracey KJ (2005) High-mobility group box 1 protein (HMGB1): nuclear weapon in the immune arsenal. Nat Rev Immunol 5(4):331–342. https://doi.org/10.1038/nri1594
14. Terrando N, Yang T, Wang X, Fang J, Cao M, Andersson U, Erlandsson HH, Ouyang W, Tong J (2016) Systemic HMGB1 neutralization prevents postoperative neurocognitive dysfunction in aged rats. Front Immunol 7:441. https://doi.org/10.3389/fimmu.2016.00441
15. Chen XH, Chen DT, Huang XM, Chen YH, Pan JH, Zheng XC, Zeng WA (2018) Dexmedetomidine protects against chemical hypoxia-induced neurotoxicity in differentiated PC12 cells via inhibition of NADPH oxidase 2-mediated oxidative stress. Neurotox Res 35(1):139–149. https://doi.org/10.1007/s12640-018-9938-7
16. Pan X, Yan D, Wang D, Wu X, Zhao W, Lu Q, Yan H (2017) Mitochondrion-mediated apoptosis induced by acrylamide is regulated by a balance between Nrf2 antioxidant and MAPK signaling pathways in PC12 cells. Mol Neurobiol 54(6):4781–4794. https://doi.org/10.1007/s12035-016-0021-1
17. Kimura S, Fujita N, Noda T, Yoshimori T (2009) Monitoring autophagy in mammalian cultured cells through the dynamics of LC3. Methods Enzymol 452:1–12. https://doi.org/10.1016/s0076-6879(08)03601-x
18. Bjorkoy G, Lamark T, Brech A, Outzen H, Perander M, Overvatn A, Stenmark H, Johansen T (2005) p62/SQSTM1 forms protein aggregates degraded by autophagy and has a protective effect on huntingtin-induced cell death. J Cell Biol 171(4):603–614. https://doi.org/10.1083/jcb.200507002
19. Kimura S, Noda T, Yoshimori T (2007) Dissection of the autophagosome maturation process by a novel reporter protein, tandem fluorescent-tagged LC3. Autophagy 3(5):452–460
20. Porter K, Nallathambi J, Lin Y, Liton PB (2013) Lysosomal basification and decreased autophagic flux in oxidatively stressed trabecular meshwork cells: implications for glaucoma pathogenesis. Autophagy 9(4):581–594. https://doi.org/10.4161/auto.23568
21. Yang YP, Hu LF, Zheng HF, Mao CJ, Hu WD, Xiong KP, Wang F, Liu CF (2013) Application and interpretation of current autophagy inhibitors and activators. Acta Pharmacol Sin 34(5):625–635. https://doi.org/10.1038/aps.2013.5
22. Lu Y, Wu X, Dong Y, Xu Z, Zhang Y, Xie Z (2010) Anesthetic sevoflurane causes neurotoxicity differently in neonatal naive and Alzheimer disease transgenic mice. Anesthesiology 112(6):1404–1416. https://doi.org/10.1097/ALN.0b013e3181d94de1
23. Zhang L, Zhang J, Yang L, Dong Y, Zhang Y, Xie Z (2013) Isoflurane and sevoflurane increase interleukin-6 levels through

the nuclear factor-kappa B pathway in neuroglioma cells. Br J Anaesth 110(Suppl 1):i82–i91. https://doi.org/10.1093/bja/aet115
24. Galluzzi L, Vicencio JM, Kepp O, Tasdemir E, Maiuri MC, Kroemer G (2008) To die or not to die: that is the autophagic question. Curr Mol Med 8(2):78–91
25. Carloni S, Buonocore G, Balduini W (2008) Protective role of autophagy in neonatal hypoxia-ischemia induced brain injury. Neurobiol Dis 32(3):329–339. https://doi.org/10.1016/j.nbd.2008.07.022
26. Martinez-Vicente M (2015) Autophagy in neurodegenerative diseases: from pathogenic dysfunction to therapeutic modulation. Semin Cell Dev Biol 40:115–126. https://doi.org/10.1016/j.semcdb.2015.03.005
27. Chen G, Ke Z, Xu M, Liao M, Wang X, Qi Y, Zhang T, Frank JA, Bower KA, Shi X, Luo J (2012) Autophagy is a protective response to ethanol neurotoxicity. Autophagy 8(11):1577–1589. https://doi.org/10.4161/auto.21376
28. Xiong J, Kong Q, Dai L, Ma H, Cao X, Liu L, Ding Z (2017) Autophagy activated by tuberin/mTOR/p70S6K suppression is a protective mechanism against local anaesthetics neurotoxicity. J Cell Mol Med 21(3):579–587. https://doi.org/10.1111/jcmm.13003
29. Komita M, Jin H, Aoe T (2013) The effect of endoplasmic reticulum stress on neurotoxicity caused by inhaled anesthetics. Anesth Analg 117(5):1197–1204. https://doi.org/10.1213/ANE.0b013e3182a74773
30. Li G, Yu B (2014) Elevation of protective autophagy as a potential way for preventing developmental neurotoxicity of general anesthetics. Med Hypotheses 82(2):177–180. https://doi.org/10.1016/j.mehy.2013.11.032
31. Kong ZH, Chen X, Hua HP, Liang L, Liu LJ (2017) The oral pretreatment of glycyrrhizin prevents surgery-induced cognitive impairment in aged mice by reducing neuroinflammation and alzheimer's-related pathology via HMGB1 inhibition. J Mol Neurosci 63(3–4):385–395. https://doi.org/10.1007/s12031-017-0989-7
32. Wang W, Chen X, Zhang J, Zhao Y, Li S, Tan L, Gao J, Fang X, Luo A (2016) Glycyrrhizin attenuates isoflurane-induced cognitive deficits in neonatal rats via its anti-inflammatory activity. Neuroscience 316:328–336. https://doi.org/10.1016/j.neuroscience.2015.11.001
33. Zhu X, Messer JS, Wang Y, Lin F, Cham CM, Chang J, Billiar TR, Lotze MT, Boone DL, Chang EB (2015) Cytosolic HMGB1 controls the cellular autophagy/apoptosis checkpoint during inflammation. J Clin Investig 125(3):1098–1110. https://doi.org/10.1172/jci76344
34. Kornblit B, Munthe-Fog L, Madsen HO, Strom J, Vindelov L, Garred P (2008) Association of HMGB1 polymorphisms with outcome in patients with systemic inflammatory response syndrome. Crit Care 12(3):R83. https://doi.org/10.1186/cc6935
35. Tang D, Kang R, Livesey KM, Cheh CW, Farkas A, Loughran P, Hoppe G, Bianchi ME, Tracey KJ, Zeh HJ 3rd, Lotze MT (2010) Endogenous HMGB1 regulates autophagy. J Cell Biol 190(5):881–892. https://doi.org/10.1083/jcb.200911078
36. Wang K, Huang J, Xie W, Huang L, Zhong C, Chen Z (2016) Beclin1 and HMGB1 ameliorate the alpha-synuclein-mediated autophagy inhibition in PC12 cells. Diagn Pathol 11:15. https://doi.org/10.1186/s13000-016-0459-5
37. Guan Y, Li Y, Zhao G, Li Y (2018) HMGB1 promotes the starvation-induced autophagic degradation of alpha-synuclein in SH-SY5Y cells Atg 5-dependently. Life Sci 202:1–10. https://doi.org/10.1016/j.lfs.2018.03.031
38. Erlich S, Shohami E, Pinkas-Kramarski R (2006) Neurodegeneration induces upregulation of Beclin 1. Autophagy 2(1):49–51
39. Marquez RT, Xu L (2012) Bcl-2:Beclin 1 complex: multiple, mechanisms regulating autophagy/apoptosis toggle switch. Am J Cancer Res 2(2):214–221
40. Huebener P, Gwak GY, Pradere JP, Quinzii CM, Friedman R, Lin CS, Trent CM, Mederacke I, Zhao E, Dapito DH, Lin Y, Goldberg IJ, Czaja MJ, Schwabe RF (2014) High-mobility group box 1 is dispensable for autophagy, mitochondrial quality control, and organ function in vivo. Cell Metab 19(3):539–547. https://doi.org/10.1016/j.cmet.2014.01.014

Publisher's Note Springer Nature remains neutral with regard to jurisdictional claims in published maps and institutional affiliations.